Electronic Supplementary Material for Chemical Communications

Photosensitive gelatin

Ana Vesperinas, [a] Julian Eastoe,*[a] Paul Wyatt,[a] Isabelle Grillo[b] and Richard K. Heenan[c]

[a] *School of Chemistry, University of Bristol, Bristol, BS8 1TS, UK.Fax:+44 117 9250612;Tel:+44 117 9289180; E-mail: julian.eastoe@bristol.ac.uk*
[b] *Institut Max-von-Laue-Paul-Langevin, BP 156-X, F-38042, Grenoble, Cedex, France.*
[c] *ISIS Rutherford Appleton Laboratory ,Chilton, Oxon, OX11 0QX,UK.*

Supporting Information

C6PAS photochemistry

Photolysis of Sodium 4-hexylphenylaosulfonates (C6PAS) can be achieved by UV irradiation. The photochemistry of C6PAS proposed by Nuyken and Voit,[1] follows a radical or an ionic mechanism forming either alkylbencene or 4-alkylphenol, depending on the environment. In sufficiently concentrated aqueous systems, both mechanisms compete.[1,2]

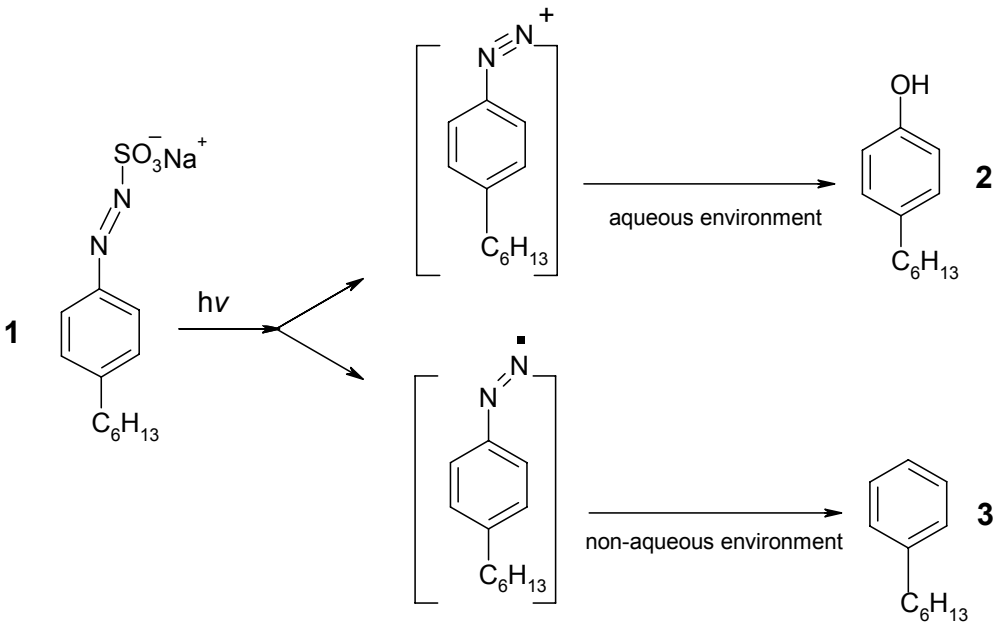

Scheme S1. Photochemical degradation pathways for the surfactant (**1**) C6PAS, yielding hexyl-4-phenol (**2**) and/ or hexylbenzene (**3**).

As is described in the main paper, surfactant micelles are bound to cationic gelatin strands by electrostatic forces.[3]

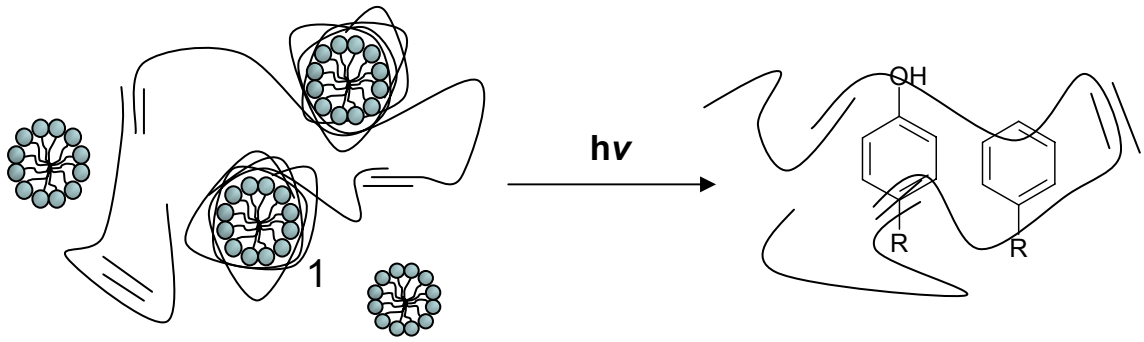

Scheme S2. Concept of UV changes in surfactant micelle-gelatin binding. Generation of photoproducts affects the association of the surfactant-gelatin network.

UV-Vis spectra

C6PAS/gelatin samples displayed an intense UV absorption at λ 308 nm characteristic of the C6PAS photosurfactant.[2] After irradiation (carried out in a quartz cell, with an Oriel unfiltered 100W high-pressure white source) this characteristic peak disappeared, suggesting that the photoreaction is complete.

The C6PAS-surfactant gelatin complexes (SGC's) at 8 mM C6PAS in 5 wt% gelatin took 65 min for completion of the photodegradation, as monitored by UV-Vis spectroscopy. This was longer than for the equivalent gelatin-free sample (27 min), perhaps owing to strong surfactant binding in the SGC system hindering the photolysis.

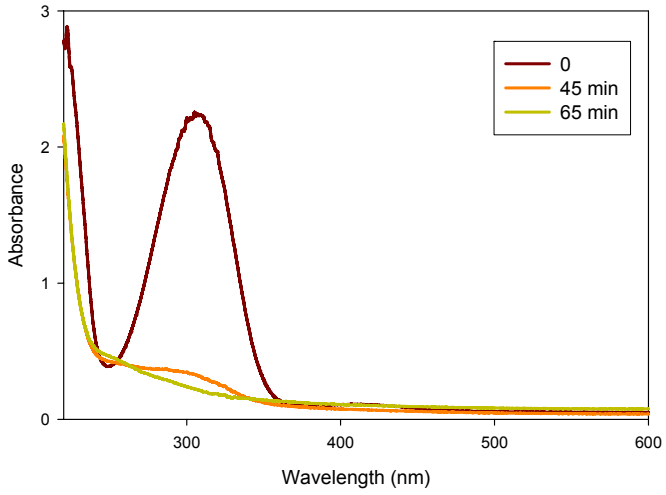

Figure S1. UV-Vis spectra of 0.008M C6PAS/5 wt% Gelatin

Small-Angle Scattering Analysis

Small-angle neutron scattering is a diffraction-type technique, normally employing incident beams of $\lambda \sim 1 - 10$ Å, to reveal structural features (inhomogeneities) on length scales 10 - 1000Å. See www.isis.ac.uk/largescale, www.ill.fr and www.chm.bris.ac.uk/pt/eastoe/EastoeHome.htm. SANS experiments were carried out at the D22 diffractometer at ILL (Grenoble, France) using a neutron wavelength of λ = 10 Å at two different detector distances to cover a Q range of 0.0024 $\rightarrow$ 0.37 Å $^{-1}$. Absolute intensities for I(Q) (cm^{-1}) were determined to within $\pm$ 5% by measuring the incoherent scattering from 1 mm of H_2O. Measurements were conducted in 2 mm rectangular quartz cells, at 41°C. Samples for SANS were prepared using D_2O and different concentrations of C6PAS in 5% and 10% gelatin. The data were all analyzed using the FISH program.[4]

Gelatin solutions

For the gelatin scattering a scattering law has proposed given by Pezron et al.[5]. They considered two contributions to the total intensity:

$$I(Q)=I_{Lorentz}(Q) + I_{ex}(Q) \qquad \text{(Eq. S1)}$$

The Lorentzian component can be described as:

$$I_{Lorentz}(Q) = \frac{I(0)}{1+Q^2\xi^2} \qquad \text{(Eq. S2)}$$

Where ξ is the average mesh size of the transient network of chains.

To account for the deviation at low angles from the Lorentzian shapes, an excess scattering $I_{ex}(Q)$ term, is employed from Debye-Bueche theory, which takes in consideration contributions from inhomogeneities (owing to strand-strand interactions).

$$I_{ex}(Q) = \frac{I_{ex}(0)}{(1+Q^2a^2)^2} \qquad \text{(Eq. S3)}$$

where a is a measure of the inhomogeneity domain size.

Plotting the inverse scattered intensities $(I(Q))^{-1}$ as a function of Q^2, in the range of $8\times10^{-3} \leq Q \leq 2\times10^{-2}$ Å^{-1}, a linear dependence is expected, the slope allows calculation of ξ. At small Q vectors in the range $8\times10^{-3} \leq Q$ the excess scattering factor is apparent (downward curvature) as a deviation from the linear fit (Figure S2).

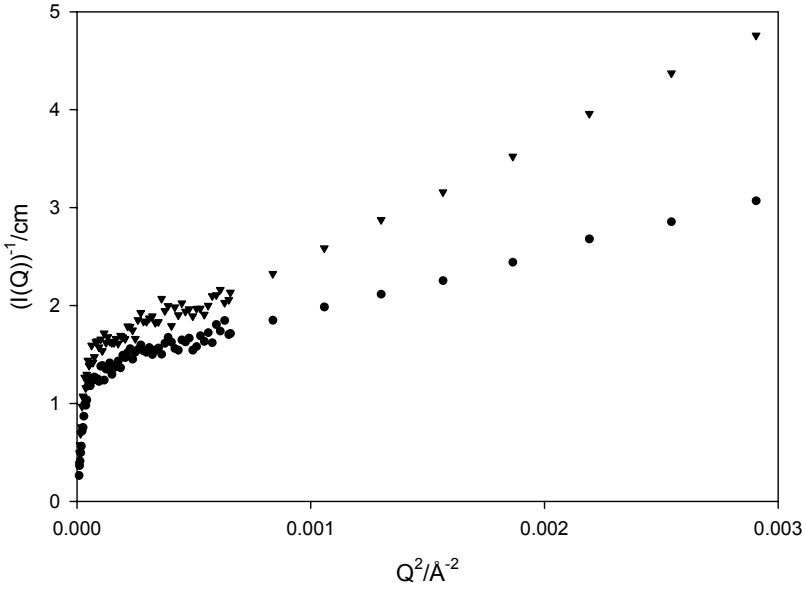

Figure S2. Inverse scattered intensities $(I(Q))^{-1}$ versus Q^2 for 5 wt% (●) gelatin and 10 wt% gelatin (▼) in D_2O.

The characteristic inhomogeneity domain sizes have been approximated from the slope of $(I(Q))^{-1/2}$ versus Q^2 to give a. The values are very close to those obtained by fitting the full scattering law (Table S1).

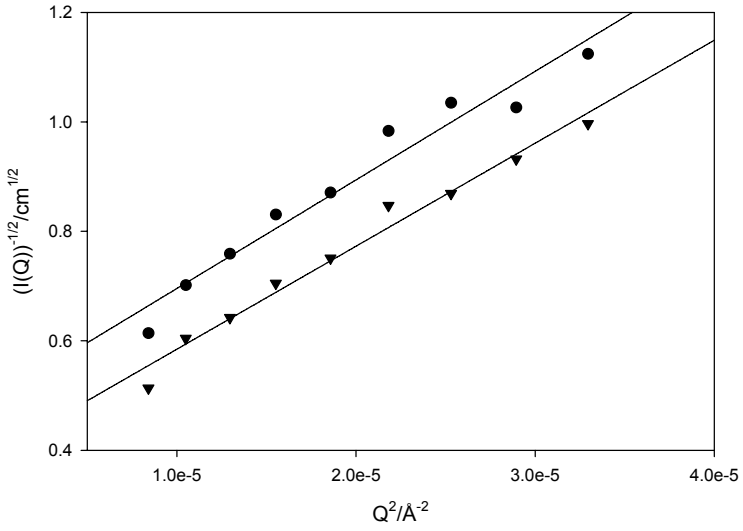

Figure S3. Excess scattering according to the Debye-Bueche model. At low Q a linear dependence for $(I(Q))^{-1/2}$ versus Q^2 is observed, the slopes give a for 5 wt% (●) gelatin and 10 wt% gelatin (▼).

Data from the fits using model Lorentz plus Debye-Bueche are in aggrement with Pezron[5], and with the values obtained form the slope analysis based on limiting behaviour.

wt% gelatin	Limiting low		Scattering low	
	ξ (Å)	a (Å)	ξ (Å)	a (Å)
5	35	154	34.4	154
10	27.3	172.6	25.4	172

Table S1. Average mesh size ξ for gelatin (Lorentzian behaviour) and size of inhomogeneities a (Debye/Bueche contribution).

C6PAS in solution

Detailed analysis of SANS aqueous micelles of C6PAS, alone and in combination with an inert non-ionic surfactant have been previously reported.[6] For pure C6PAS before irradiation SANS data were consistent with small charged micelles, fitted using the Hayter and Penfold model.[7] The normalised SANS intensity I(*Q*) for globular ionic micelles may be written as,

$$I(Q) = NP(Q)S(Q) \qquad \text{(Eq. S4)}$$

Where the scattered intensity I(*Q*) is not only determined by a form factor P(*Q*), but also by a structure factor S(*Q*) arising from inter-particle interactions.

For globular charged micelles the form factor is related with the size-averaged scattering function.[8]

$$P(Q) = \left\langle F(Q)^2 \right\rangle \qquad \text{(Eq. S5)}$$

where $F(Q)$ is the single particle form factor which depends on the size and shape of the particle, $F(Q)$ for anisotropic micelles (e.g. ellipsoidal)

$$\left\langle F(Q)^2 \right\rangle = \int_0^1 [F(Q,\mu)^2 \, d\mu] \qquad \text{(Eq. S6)}$$

$$\left\langle F(Q) \right\rangle^2 = \left[\int_0^1 F(Q,\mu) d\mu \right]^2 \qquad \text{(Eq. S7)}$$

$$F(Q,\mu) = 3(\sin\omega - \omega\cos\omega)/\omega^3, \qquad \text{(Eq. S8)}$$

where $\omega = Q[a^2\mu^2 + x^2(1-\mu^2)]^{1/2}$, (a and c are, respectively, the semi-minor and semi-major axes of ellipsoid of revolution while μ is the cosine of the angle between the direction of c and Q).

The interparticle structure factor $S(Q)$ specifies the correlation between the micelle centres. $S(Q)$ has been evaluated analytically for charged spherical particles by Hayter and Penfold[7] using the mean spherical approximation (MSA) as:

$$S(Q\sigma) = \frac{1}{1 - 24\eta\left(\dfrac{\gamma\exp(-\kappa\sigma)(\kappa\sigma\sin Q\sigma + Q\sigma\cos Q\sigma)}{Q\sigma[(Q\sigma)^2 + (\kappa\sigma)^2]} \right)} \qquad \text{(Eq. S9)}$$

where κ is the Debye-Hückel inverse screening length, σ is the diameter of the macroion and η is volume fraction.

This model describes well SANS from charged colloidal particles interacting through a screened Coulomb potential, at moderate to high densities. The rescaled mean spherical approximation (RMSA) applies at lower densities.[9]

Prior to irradiation the scattering profiles and intensities for pure C6PAS change progressively with increasing photosurfactant concentration

(Figure S4). The ellipsoidal micelles become more spherical and an increase in charge is noticeable based on fitted values given in Table S2.

Non irradiated

[C6PAS]/mM	R_1(Å)	R_2(Å)	Charge α
40	15.2	9.4	9
60	16.1	9.6	9
80	14.1	14.8	27

Table S2. Parameters fitted to SANS data shown in Figure S4.

Irradiated C6PAS

Initially a study of post–irradiated systems of pure C6PAS alone was carried out for concentrations 40 mM and 20 mM. The curves displayed a very strong Q^{-4} scattering and fitting of these SANS profiles could not be achieved by any simple or physically reasonable scattering low. For the most concentrated irradiated samples a strong logarithmic dependence with Q^{-3} scattering is present in most of the Q range; these data could be interpreted using a model proposed by Kotlarchyk.[10]

This Kotlarchyk model assumes a randomly oriented assembly of lamellar microdomains or stacks, with relative scattering-length density variation ($\Delta\rho$) along one of the *z* axis, attenuated by a Gaussian profile $\exp(-z^2/2\sigma^2)$. The characteristic interfacial thickness is given by $t=(2\pi)^{1/2}\sigma$ and the absolute scattered intensity from a particle of thickness *D* containing n_s randomly oriented stacks per unit volume is given by:

$$I(Q) = NP(Q,\mu)S^{'}(Q,\mu) \qquad \text{(Eq. S10)}$$

μ is the cosine of the angle between the scattering vector *Q* and the *z* axis define by the stack. Equation S10 can be simplified with:

$$I(Q) = L_N(Q)P(Q,\mu=1)S'(Q,\mu=1) \qquad \text{(Eq. S11)}$$

when $R\sigma$ is large the Lorentz factor can be approximated to:

$$L_N(Q) = \frac{1}{1 + \frac{1}{2}Q^2(R\sigma)^2} \qquad \text{(Eq. S12)}$$

If Rσ=0 the Q vector is normal to the surface, i.e. the interface is perfectly flat.

Photolysis generated insoluble oily photoproducts (Scheme S1), which phase separate from the majority aqueous portion of the sample. Therefore, it would be expected that the effective volume fraction (ϕ) of hydrocarbon chains decreases dramatically after irradiation. Comparison of fitted scale factors for the pre- and post-irradiated samples at 80 mM C6PAS is consistent with this photoseparation (before UV ϕ=2.5%, after UV ϕ=0.07%).

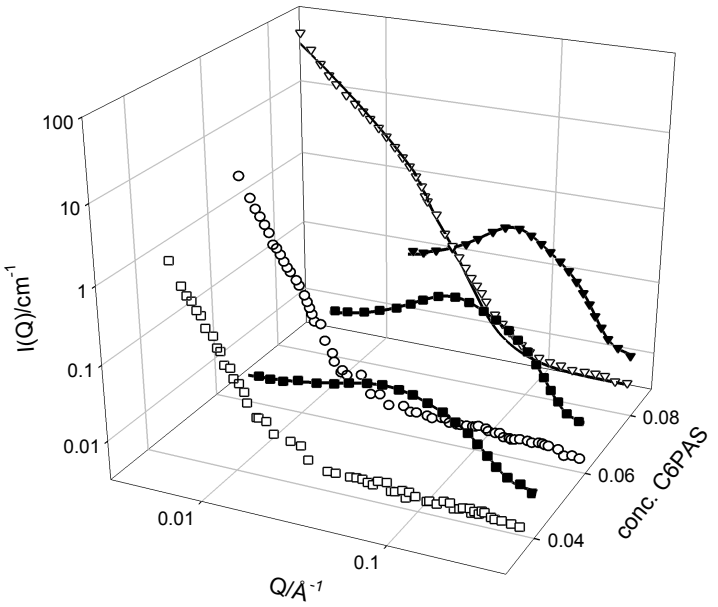

Figure S4. SANS data and model fitting analyses for C6PAS/D_2O solutions. Before irradiation filled, and after irradiation empty markers.

Non-irradiated Gelatin/C6PAS mixtures

Figure S5 shows SANS fits for C6PAS-SGC's at 10% gelatin solutions and different surfactant concentrations. For interacting systems of globular charged micelles, the SANS can be fitted using the Hayter and Penfold model[4] as has been used to fit C6PAS/D_2O solutions described above.

Prior to irradiation the scattering profile changes progressively with surfactant concentration (Table S3). The ellipsoidal micelles became smaller and less charged with C6PAS concentration.

Irradiated C6PAS/Gelatin mixtures

SANS from irradiated C6PAS displays a strong logarithmic dependence, which can be fitted using the Kotlarchyk[10] model described above. Irradiation of C6PAS-SGC's results in a destruction of the C6PAS micelles; this strongly affects the gelatin structure since two insoluble photoproducts are formed. These seem to weakly associate with gelatin (rather than phase separate) forming large aggregates, which can be interpreted as polydisperse sheets of thickness *t*. As shown in Table S3 the apparent thickness increases with C6PAS concentration, as fraction of photoproducts increase.

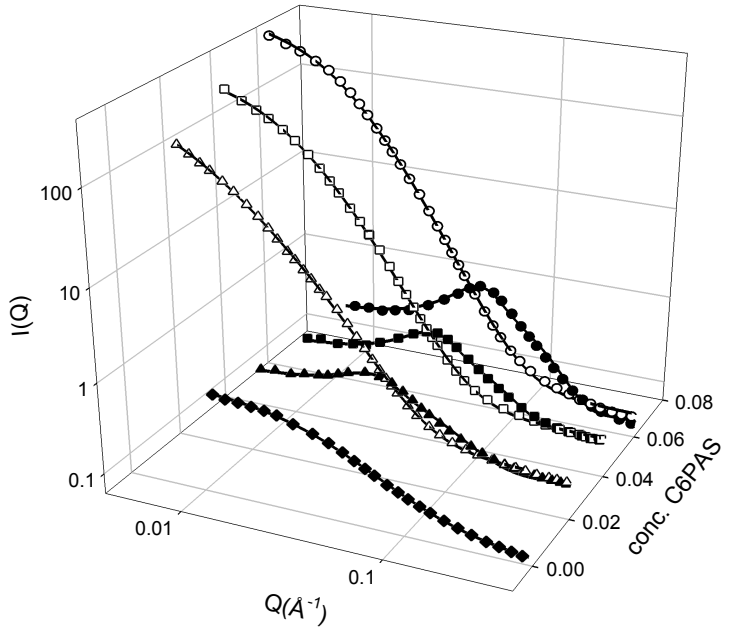

Figure S5. SANS data from 10 wt% gelatin C6PAS-SGC's before (filled markers) and after irradiation (empty markers).

Non irradiated

[C6PAS]/mM	R_1 (Å)	R_2 (Å)	Charge α
20	16.0	79.4	38
40	15.8	62.2	24
60	15.1	57.6	22

UV irradiated

[C6PAS]/mM	*t* (Å)
20	74
40	152
60	242

Table S3 Parameters fitted to SANS data shown in Figure S5.

References

1 O. Nuyken and B. Boiy, *Macromol. Chem. Phys.,* 1997, **198**, 2337

2. T. Mezger, O. Nuyken, K. Meindl, A. Wokaun, *Progr. in Org. Coatings* 1996, **29**, 147.

3. T. Cosgrove, S. J. White, A. Zarbakhsh, *Lamgmuir*, 1995, **11**, 744.

4. R. K. Heenan, Fish Data Analisys Program; Report RAL-89-129, Rutherford Appleton Laboratory, CCLRC: Didcot U.K. 1989.

5. I. Pezron, M. Djabourov, J. Leblond, *Polymer* 1991, **32**, 3200.

6. A. Vesperinas, J. Eastoe, P. Wyatt, I Grillo, R. K. Heenan, J. M. Richards, G. A. Bell, *J. Am. Chem. Soc.* 2006, **128(5)**, 1468.

7. J. B. Hayter, J. Penfold, *Mol. Phy.* 1981, **42**, 109.

8. M. Kotlarchyk, S. H. Chen, *J. Chem. Phys.* 1983, **79**, 2461.

9. J.P. Hansen, J.B. Hayter, *Mol. Phys.* 1982, **46**, 651.

10. M. Kotlarchyk, S. M. Ritzau, *J. Appl. Cryst* 1991, **24**, 753.